Dalton Transactions

Accepted Manuscript

ROYAL SOCIETY OF CHEMISTRY

www.rsc.org/dalton

Journal Name

ARTICLE

Interaction of Gd-DTPA with phosphate and phosphite: Toward the reaction intermediate in Nephrogenic Systemic Fibrosis

Received 00th January 20xx,
Accepted 00th January 20xx

DOI: 10.1039/x0xx00000x

www.rsc.org/

Song Gao[a], Simon J. George[b], Zhao-Hui Zhou[a*]

Direct reactions of MRI contrast agent $K_2[Gd(DTPA)(H_2O)]\cdot 5H_2O$ (**1**) (H_5DTPA = diethylenetriaminpentaacetic acid) with dipotassium hydrogen phosphate (K_2HPO_4) or phosphite (K_2HPO_3) result in the isolations of well-defined Gd-DTPA phosphite $K_6[Gd_2(DTPA)_2(HPO_3)]\cdot 7H_2O$ (**2**) or phosphate $K_6[Gd_2(DTPA)_2(HPO_4)]\cdot 10H_2O$ (**3**), respectively. Their lanthanum analogs $K_4[La_2(DTPA)_2(H_2O)]\cdot 8H_2O$ (**4**), $K_6[La_2(DTPA)_2(HPO_3)]\cdot 7H_2O$ (**5**) and $K_6[La_2(DTPA)_2(HPO_4)]\cdot 10H_2O$ (**6**) are used for comparisons. The phosphate and phosphite groups are able to substitute the coordinated water molecules in **1** and **4** in a close physiological aqueous solution, and act as bridging ligands to link adjacent $Ln(DTPA)^{2-}$ (Ln = Gd and La) into dimeric structures. Solid state and solution ^{13}C NMR spectra of dimer **4** show the full dissociation into monomeric species in solution, while no dissociation is observed for lanthanum phosphite **5** and phosphate **6** in solution, which show only one set of ^{13}C spectra with the largest downfield shifts at 182.0 and 182.3 ppm respectively. Comparisons of the bond distances and spectral data indicate that the interaction between DTPA and central Ln^{3+} cations are weakened after the substitutions, which support that phosphate substituted Gd-DTPA as an initial intermediate in nephrogenic systemic fibrosis.

Introduction

Gadolinium, located in the middle of lanthanide elements, is widely applied in magnetic resonance imaging (MRI) as a contrast agent (CA) because of its unique magnetic properties. Since the first modern CA of Gd-DTPA (H_4DTPA = diethylenetriaminepentaacetic acid) was approved in 1988,[1] the gadolinium based contrast agents (GBCAs) have been intensively studied and clinically widely used. In GBCAs, Gd atoms are coordinated by strong chelating ligands in order to obtain high water solubility and *in vivo* stability as well as eliminating the toxicity of free Gd(III).[2] Nowadays, it is estimated that about 35% of MRI exams are performed with the use of CAs.[3] Although the other types of contrast agents have been investigated,[4] GBCAs remain the dominant agents in MRI procedures.

The clinically used GBCAs, like the commonly used Gd-DTPA (commercial name Magnevist®), were generally thought to be safe even in patients with impaired renal function. However, in 1997 (reported in 2000) a rare but potentially fatal disease, nephrogenic systemic fibrosis (NSF), was identified,[5] which was subsequently confirmed to be associated with exposure to GBCAs as the disease was found exclusively in patients who had been injected with GBCAs and who were suffering with renal failure.[6] The link with GBCAs was strengthened by scanning electron microscopy/energy dispersive spectroscopy (SEM/EDS) measurements which showed that insoluble micron–sized deposits containing Gd together with Ca, K, Na were present in the affected tissues of NSF patients.[7] Synchrotron X-ray fluorescence (SXRF) microscopy on these deposits revealed a clear quantitative correlation between Gd, Ca and P and NSF. Extended X-ray absorption fine structure (EXAFS) spectroscopy indicated that the deposits contain of $GdPO_4$ salts, in which the Gd−P distances at 3.11 Å and 3.72 Å as well as Gd−Gd distances at an average of 4.05 Å.[8] Critically, the EXAFS showed no evidence that the DTPA chelate was still present.[8] Since GBCAs are the only significant Gd source in the human body, the clear implication is that Gd(III) has been somehow liberated from the GBCA chelate, which finally causes NSF. So far there is still no effective therapy for the NSF disease.[9]

The mechanism by which Gd(III) subsequently incorporated into these insoluble $GdPO_4$ deposits is not understood. The biological safety of GBCAs was guaranteed by the high thermodynamic stability and kinetic inertness of the chelate.[2] Previous studies have generally supposed that the transmetalation causes the release of Gd(III) cations from the stable Gd chelates,[10] and also the association with phosphate and the substitution of Gd complexes with model compounds of ethylenediaminetetraacetates.[11]

In this paper, the most representative complex Gd-DTPA was chosen as a model compound of GBCAs. In aqueous solutions close to physiological pH, the interaction of

[a] State Key Laboratory of Physical Chemistry of Solid Surfaces, College of Chemistry and Chemical engineering, Xiamen University, Xiamen, 361005, China.
[b] Department of Chemistry, University of California, Davis, CA 95616, United States.

† Footnotes relating to the title and/or authors should appear here.
Electronic Supplementary Information (ESI) available: Experimental section (including Experimental details, analytical and characterization data of **1**~**6**), detailed crystal data and selected bond distances of **1**, **2** and **4**~**6**, IR spectra of **4** and **5** and H_5DTPA, ^{13}C NMR spectrum of K_5DTPA and ^{31}P NMR spectrum of **5**. See DOI: 10.1039/x0xx00000x

$K_2[Gd(DTPA)(H_2O)]\cdot 5H_2O$ (**1**) with both phosphite and phosphate salts were studied, which finally result in the formations of substituted products Gd-DTPA-HPO_3 (**2**) and Gd-DTPA-HPO_4 (**3**). For comparison, we studied the analogous lanthanum complexes: La-DTPA-H_2O (**4**), La-DTPA-HPO_3 (**5**) and La-DTPA-HPO_4 (**6**) and in these cases extended the characterization using solution and solid state NMR spectroscopy.

Results and discussion

Previous isolations and structural analyses of lanthanide phosphates were limited except for the several natural minerals and high temperature products.[12] This is due to the lanthanide phosphates generally precipitate rapidly into less ordered and insoluble phases.[13] It proceeds more quickly under the circumstances similar to the mild and close physiological conditions, where the Gd-DTPA is speculated to transform into the $GdPO_4$-like salts. In this study, parallel experiments of Gd-DTPA with phosphite and phosphate were performed. Mixed-ligand complex $K_6[Gd_2(DTPA)_2(HPO_3)]\cdot 7H_2O$ (**2**) was isolated at 40°C by the substitution of $K_2[Gd(DTPA)(H_2O)]\cdot 5H_2O$ (**1**) with H_3PO_3 at pH 7.4. Similarly, $K_6[Gd_2(DTPA)_2(HPO_4)]\cdot 10H_2O$ (**3**) was obtained by the substitution with K_2HPO_4. The former HPO_3^{2-} is considered as less steric hindrance group compared with HPO_4^{2-}. Similar reactions of $K_4[La_2(DTPA)_2(H_2O)]\cdot 8H_2O$ (**4**) with HPO_3^{2-} and HPO_4^{2-} result in the formations of mixed-ligand complexes of $K_6[La_2(DTPA)_2(HPO_3)]\cdot 7H_2O$ (**5**) and $K_6[La_2(DTPA)_2(HPO_4)]\cdot 10H_2O$ (**6**).

Crystal structure descriptions

The anion structure of $K_2[Gd(DTPA)(H_2O)]\cdot 5H_2O$ (**1**) is similar to the reported structure of MRI contrast agent Gd-DTPA as shown in Fig. 1.[14] The central Gd(III) is nona-coordinated by five carboxy oxygen atoms and three nitrogen atoms from DTPA ligand, and one coordinated water molecule. While the lanthanum complex $K_4[La_2(DTPA)_2(H_2O)]\cdot 8H_2O$ (**4**) forms a dinuclear structure by sharing a pair of carboxy oxygen atoms in both DTPA ligand as shown in Fig. 2. Only one coordinated water molecule locates on one side of the La(III) cations, therefore this La(III) is deca-coordanated while the other La(III) without coordinated water molecule is nona-coordinated. However, as we will discuss later in NMR section, the dimeric complex **4** will dissociate into monomeric species like **1** after dissolving in solution.

In neutral solution, the reaction of H_3PO_3 with Gd-DTPA-H_2O (**1**) results in the formation of the mixed-ligand complex $K_6[Gd_2(DTPA)_2(HPO_3)]\cdot 7H_2O$ (**2**). It is worth to note that **2** is formed by the substitution of HPO_3^{3-} group with the coordinated water molecule in **1**. As shown in Fig. 3, the HPO_3^{2-} acts as a bridging ligand to link the adjacent $[Gd(DTPA)]^{2-}$ in the mode of Gd−O−P−O−Gd into a dimeric structure. Central Gd(III) cation is nona-coordinated by the $DTPA^{5-}$ and an oxygen atom from HPO_3^{2-}. The bridging HPO_3^{2-} group in **2** exists in alternative symmetric orientations. The anion structure of $K_6[La_2(DTPA)_2(HPO_3)]\cdot 7H_2O$ (**5**) is shown in Fig. S1, which is obtained similarly from the reaction of H_3PO_3 with La-DTPA-H_2O (**4**). Both **2** and **5** consist of the anionic dinuclear unit of $[Ln_2(DTPA)_2(HPO_3)]^{6-}$ (Ln = Gd **2**; La **5**).

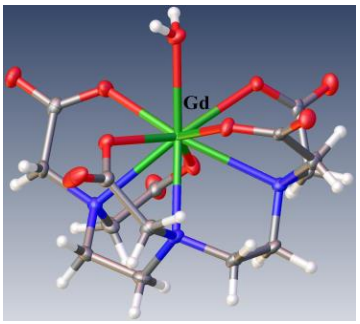

Fig. 1 Olex2 plot of the anionic structure in $K_2[Gd(DTPA)(H_2O)]\cdot 5H_2O$ (**1**) (Green, Gd; Red, O; Blue, N; Grey, C; White, H).

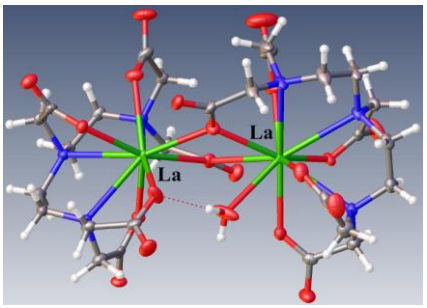

Fig. 2 Olex2 plot of the anionic structure in $K_8[La_2(DTPA)_2(H_2O)]_2\cdot 16H_2O$ (**4**) (Green, Gd; Red, O; Blue, N; Grey, C; White, H).

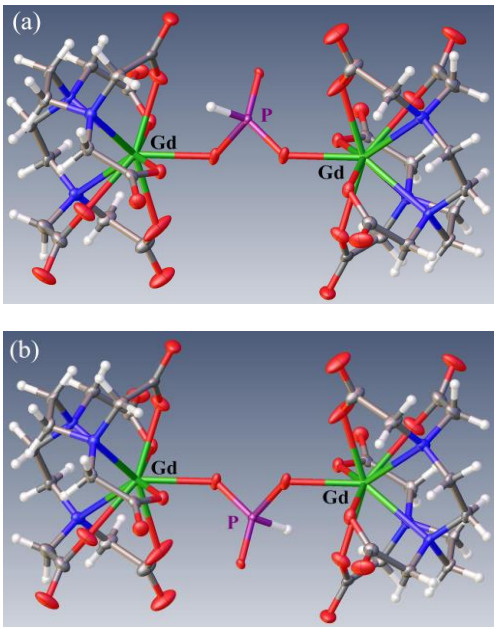

Fig. 3 Olex2 plot of the anionic structures in $K_6[Gd_2(DTPA)_2(HPO_3)]\cdot 7H_2O$ (**2**) and the alternative symmetric orientations of HPO_3^{2-} group. (Green, Gd; Red, O; Blue, N; Grey, C; White, H).

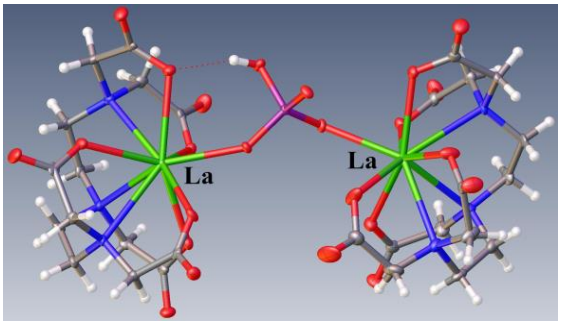

Fig. 4 Olex2 plot of the anionic structure in $K_6[La_2(DTPA)_2(HPO_4)]\cdot 10H_2O$ (**6**) (Green, La; Red, O; Blue, N; Grey, C; White, H).

The substitutions of the coordinated water molecules in Gd-DTPA-H_2O (**1**) and La-DTPA-H_2O (**4**) with HPO_4^{2-} result in the formations of $K_6[Gd(DTPA)(HPO_4)]\cdot 10H_2O$ (**3**) and $K_6[La(DTPA)(HPO_4)]\cdot 10H_2O$ (**6**) respectively. As shown in Fig. 4, complex **6** consists of a dimeric $La_2(DTPA)_2(HPO_4)^{6-}$ anion, in which HPO_4^{2-} acts as a bridging ligand connecting adjacent La-DTPA units by two phosphoric oxygen atoms. The other two free oxygen atoms are fixed by potassium cations. Moreover, it is interesting to note that one of the free oxygen atoms is protonated and forms a strong hydrogen bond with a carboxy group O19 (O23···O19 2.751 Å). The hydrogen bond plays an important role in stabilizing the coordinated HPO_4^{2-} group. Both of the La(III) cations are nona-coordinated. The integral molecule of **6** still contains potassium cations and crystal water molecules. Unfortunately, attempt to obtain the crystal of **3** is unsuccessful. While based on the comparisons of element analyses and IR spectra, it is considered that the structure of mixed Gd-DTPA-HPO_4 (**3**) is similar with lanthanum La-DTPA-HPO_4 (**6**).

Selected average bond distances of **1**, **2** and **4** ~ **6** are listed in Table 1. The comparisons of these bond distances indicated that: Firstly, the Gd−$O_{phosphite}$ distance [2.320(8) Å] in Gd-DTPA-HPO_3 (**2**) is obvious shorter than that of Gd−O_{water} [2.448(2) Å] in Gd-DTPA-H_2O (**1**). The short and strong bond indicates that the HPO_3^{2-} group is favorable for the substitution of coordinated water molecule in Gd-DTPA-H_2O (**1**). It suggests that the bond strength of Gd−$O_{phosphite}$ is more stable than that of Gd−O_{water}. Secondly, the average Gd−$O_{carboxy}$ bond distance of **2** is 2.417(8) Å, which is comparable with that of **1** [2.391(2) Å]. Similar result is found in the Gd−N distances, where the average Gd−N distance of **2** is 2.683(7) Å, similar to that of 2.659(2) Å in **1**, but they seem a little longer. From which we can observe the increasing bond distances of Gd (III) with DTPA ligand from **1** to **2**. The complexation of DTPA chelate with central Gd(III) is weakened as a result of the substitution of coordinated water molecule with phosphite.

In the lanthanum complexes **4**, **5** and **6**, the bond distances of La−$O_{phosphate}$ [2.449(2) Å, **6**] and La−$O_{phosphite}$ [2.428(5) Å, **5**] are obviously shorter than that of La−O_{water} [2.674(5) Å, **4**], which suggests that both of HPO_4^{2-} and HPO_3^{2-} are better substitutive groups compared with the coordinated water molecule. Contrarily, the La–$O_{carboxy}$ bond distances in **5** and **6** appear to be shorter than those in **4**, which do not agree with the changes in Gd–$O_{carboxy}$. This is mainly caused by the dimeric structure of La-DTPA-H_2O (**4**), in which there are two carboxy groups shared by the adjacent $La(DTPA)^{2-}$ units leading to the weakening of the coordination strength with central La(III). However, after dissolved in aqueous solution, **4** would not maintain its dimeric structure, but dissociated into a monomeric structure like Gd-DTPA-H_2O (**1**). This will be discussed below.

Full data of Gd−O, Gd−N, La−O and La−N bond distances in the complexes are listed in Tables S2 to S4 in the Supplementary materials.

Table 1 Comparisons of the average bond distances of Ln−O, Ln−N and Ln−P (Å), Ln = Gd **1**, **2**; La **4**, **5**, **6**).

Compounds		**1**	**2**	**4**	**5**	**6**
Ln–O(Å)	Ln–$O_{carboxy}$ (Å)	2.391(2)	2.417(8)	2.544(5)	2.520(5)	2.532(3)
	Ln−O_{water} (Å)	2.448(2)		2.674(5)		
	Ln−$O_{phosphite}$ (Å)		2.320(8)		2.428(5)	
	Ln−$O_{phosphate}$ (Å)					2.449(2)
Ln−N (Å)		2.659(2)	2.683(7)	2.844(4)	2.798(5)	2.834(3)
Ln−P (Å)			3.566		3.700	3.697

Table 2 ^{13}C NMR spectral data (in ppm) for **4**, **5**, **6** and K_5DTPA.

	Solution			Solid state		
	-CH_2N	-NCH_2CO_2	-CO_2	-CH_2N	-NCH_2CO_2	-CO_2
4	59.9, 59.4 58.7	65.7	183.5, 183.4, 182.8	54.9, 53.2	60.1, 58.4	185.4, 180.1, 178.0
5	60.8, 60.0 58.8	65.8	183.7, 183.6, 183.0	56.8	64.1	182.9, 180.7, 179.5
6	60.3, 59.0	66.0	183.9, 183.8, 183.2	57.0	66.3, 63.8	182.3, 179.6
K_5DTPA	54.1, 54.0	61.2, 60.6	181.9, 181.6			

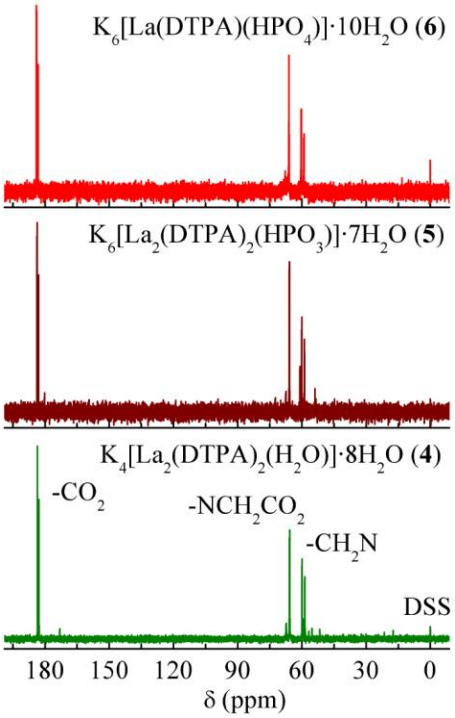

Fig. 5 Solution ^{13}C NMR spectra of $K_4[La_2(DTPA)_2(H_2O)]\cdot 8H_2O$ (**4**), $K_6[La_2(DTPA)_2(HPO_3)]\cdot 7H_2O$ (**5**) and $K_6[La_2(DTPA)_2(HPO_4)]\cdot 10H_2O$ (**6**).

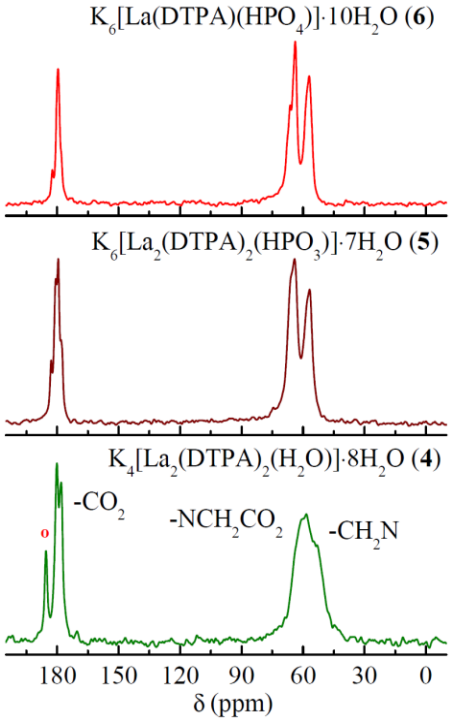

Fig.6 Solid state ^{13}C NMR spectra of $K_4[La_2(DTPA)_2(H_2O)]\cdot 8H_2O$ (**4**), $K_6[La_2(DTPA)_2(HPO_3)]\cdot 7H_2O$ (**5**) and $K_6[La_2(DTPA)_2(HPO_4)]\cdot 10H_2O$ (**6**).

NMR Analyses and solution behavior

The solution and solid state ^{13}C NMR spectra of **4** ~ **6** are shown in Figs. 5 and 6 respectively. Solution ^{13}C NMR spectrum of K_5DTPA is shown in Fig. S2. The full data is listed in Table 2, and the solution ^{13}C NMR of K_5DTPA is listed in the same table for comparison.

In the solution ^{13}C NMR spectrum of La-DTPA (**4**), the peaks at 183.5, 183.4 and 182.8 ppm correspond to carboxy groups ($-CO_2$), and those of CH_2 groups appear at 59.9, 59.4, 58.7 ($-NCH_2CO_2$) and 65.7 ($-CH_2N$) ppm respectively. Compared with K_5DTPA, obvious downfield shifts of $-CO_2$, $-NCH_2CO_2$and $-CH_2N$ indicate the coordination of $DTPA^{5-}$ ligands with central La(III) cations. What's more, solid state ^{13}C NMR data of **4** clarify its dissociation in aqueous solution. In solid state ^{13}C NMR data, the $-CO_2$ groups of **4** appear at 185.4, 180.1 and 178.0 ppm. Compared to the same groups of **5** at 182.9, 180.7, 179.5 ppm and **6** at 182.3, 179.6 ppm, it is noticeable that the peak at 185.4 ppm in **4** shows much downfield shift than the other two complexes, which can be assigned to the bridging carboxy groups that coordinated by both $La(DTPA)^{2-}$ units. However, in the solution ^{13}C NMR of **4**, the downfield peak disappears, indicating that the bridging carboxy groups no longer exist in solution. It confirms that La-DTPA-H_2O (**4**) do not keep the dimeric structure after dissolving in solution, but probably dissociates into mononuclear structure just as that in Gd-DTPA-H_2O (**1**).

The solution ^{13}C NMR of $-CO_2$ groups in La-DTPA-H_2O (**4**), La-DTPA-HPO_3 (**5**) and La-DTPA-HPO_4 (**6**) show evident regularity. Compared with **4**, the NMR peaks of $-CO_2$ groups shift downfield regularly for **5** ($\Delta\delta$ = 0.2 ppm) and **6** ($\Delta\delta$ = 0.4 ppm). It suggests the coordinated HPO_4^{2-} group is a better electron withdrawing group than HPO_3^{2-}, and HPO_3^{2-} is better than the coordinated water molecule. This is compensated by the decrease of bond strength after the formations of phosphite and phosphate.

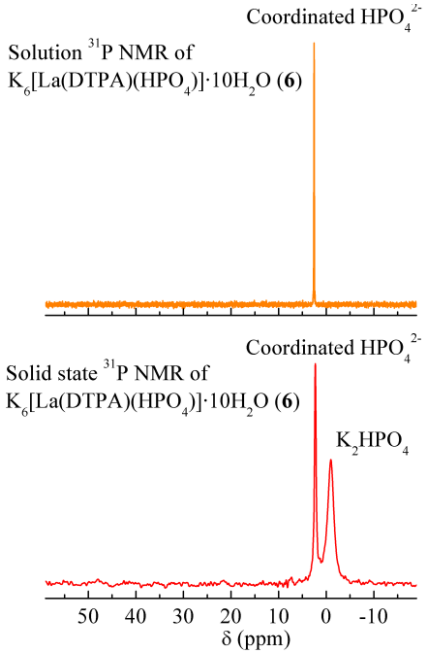

Fig. 7 Solution and solid state ^{31}P NMR spectra of $K_6[La_2(DTPA)_2(HPO_4)]\cdot 10H_2O$ (**6**), where K_2HPO_4 is added as an internal reference.

Solution and solid state ^{31}P NMR spectra of La-DTPA-HPO_4 (**6**) are shown in Fig. 7, where K_2HPO_4 salt is added as an internal reference. In the solid spectrum, downfield peak can be assigned to the coordinated HPO_4^{2-} groups, and the other one corresponds to the K_2HPO_4 salt. However, in solution ^{31}P NMR spectrum, the free and coordinated HPO_4^{2-} groups mixed together that only one single sharp peak appears. It is difficult to identify whether La-DTPA-HPO_4 (**6**) dissociates or not in solution. Similarly, the solution ^{31}P NMR spectrum of La-DTPA-HPO_3 (**5**) is shown in Fig. S3.

Vibrational spectra

IR vibrational spectra of gadolinium complexes **1** ~ **3** are overlaid in Fig. 8 (a) to show their differences. The spectra of lanthanum complexes **4** ~ **6** and H_5DTPA are shown in Figs. S4 to S7 respectively, where **6** and **3** are overlaid to highlight their similarities.

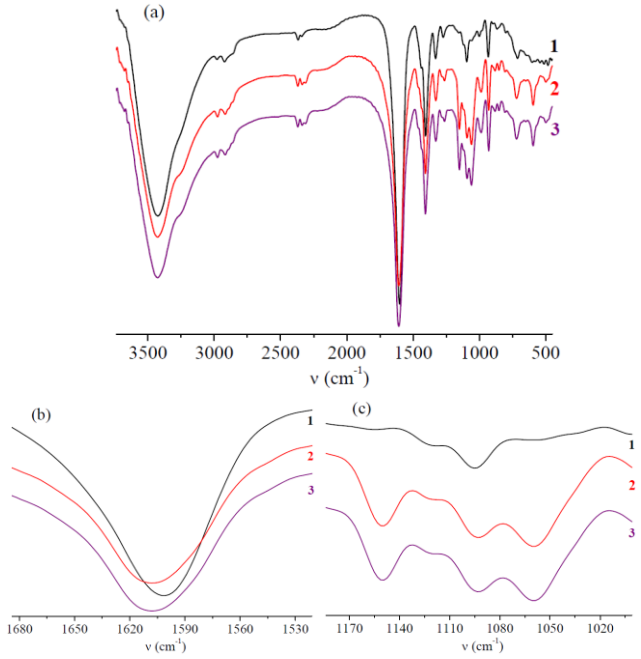

Fig. 8 IR spectra of K_2[Gd(DTPA)(H_2O)]·5H_2O (**1**), K_6[Gd_2(DTPA)$_2$(HPO_3)]·7H_2O (**2**), and K_6[Gd_2(DTPA)$_2$(HPO_4)]·10H_2O(**3**).

For **1** ~ **3**, strong peaks near 1600 cm^{-1} (**1** 1601 cm^{-1}, **2** 1606 cm^{-1}, **3** 1607 cm^{-1}) correspond to the coordinated carboxy groups of $\nu_{as}(COO^-)$ as shown in Fig. 8 (b). Compared to **1**, the substituted products **2** and **3** show red shifts of 5 and 6 cm^{-1}, respectively. The shifts may be caused by the substitution of HPO_3^{2-} or HPO_4^{2-} groups and the results in accord with the weakening of the complexation of Gd-DTPA. Middle peaks around 1400 cm^{-1} (**1** 1406 cm^{-1}, **2** 1407 cm^{-1}, **3** 1408 cm^{-1}) correspond to the $\nu_s(COO^-)$ of coordinated carboxy groups. As shown in Fig. 8 (c), the peaks at 1095 cm^{-1}, 1093 cm^{-1} and 1094 cm^{-1} correspond to the ν(C−N) vibrations for **1** ~ **3**, respectively. The other broad peaks around 1100 cm^{-1} in **2** and **3** correspond to the vibrations of P=O, among which the anti-symmetric stretching ν_{as}(P=O) appears at 1150 cm^{-1} and symmetric stretching vibration ν_s(P=O) appears at 1060 cm^{-1}. As shown in Figure S10, the IR spectra of Gd-DTPA-HPO_4 (**3**) and La-DTPA-HPO_4 (**6**) are very similar. There are slight parallel shifts caused by the lanthanide contraction, indicating similar structures of the two complexes.

Proposed transformation of Gd-DTPA to $GdPO_4$ deposits in NSF

The Gd chelates used as GBCAs, like [Gd(DTPA)(H_2O)]$^{2-}$, generally coordinate very strongly with large thermodynamic stability constant K_{GdL}, which is defined in equation (1).[2b]

$$Gd^{3+} + DTPA^{5-} \leftrightarrows [Gd(DTPA)(H_2O)]^{2-}$$

$$K_{GdL} = [Gd(DTPA)]/[Gd][DTPA] \quad (1)$$

For Gd-DTPA, the typically stability constant $K_{Gd(DTPA)}$ is 2.9×10^{22}, while it is 5.0×10^{17} at pH~7.4.[2b] In NSF, the Gd^{3+}cations of Gd-DTPA contrast agent are found precipitated as insoluble deposits of $GdPO_4$ together with Ca^{2+}, Na^+ and small amounts of other cations. The solubility constant for $GdPO_4$ [$K_{sp}(GdPO_4)$] is about 10^{-26} mol·L^{-1},[15] as is defined in equation (2).

$$GdPO_4 \leftrightarrows Gd^{3+} + PO_4^{3-}\ K_{sp} = [Gd^{3+}][PO_4^{3-}] \quad (2)$$

The concentration of serum phosphate in a person is in the range of 2.5×10^{-4} mol·L^{-1}.[7] According to the parameters above, the concentration of Gd^{3+} dissociated from $GdPO_4$ is 4.0×10^{-23} mol·L^{-1}. This is less than the dissociated concentration of Gd^{3+} in 3.2×10^{-11} mol·L^{-1} from Gd-DTPA, which is calculated based on the average amount of Gd-DTPA (Magnevist®, 5.0×10^{-4} mol·L^{-1}) used for MRI,[6] indicating the thermodynamic process for the formation of $GdPO_4$ is accessible as the following equation (3).

$$[Gd(DTPA)(H_2O)]^{2-} + PO_4^{3-} \rightarrow [Gd(DTPA)(PO_4)]^{2-}$$

$$\rightarrow GdPO_4 + DTPA^{5-} \quad (3)$$

By the reaction of free HPO_4^{2-} with [Gd(DTPA)(H_2O)]$^{2-}$, we have found that the coordinated water molecule in [Gd(DTPA)(H_2O)]$^{2-}$ is able to be substituted by HPO_4^{2-} groups, indicating the existence of the intermediate of Gd-DTPA-HPO_4 (see Scheme 1). After the substitution, it is significant to note the weakening of the Gd-DTPA complexation. The intermediate complex may further promote the precipitation of gadolinium phosphate in equation (3). The substituted product of Gd-DTPA-HPO_4 gives a new possible mechanism for the $GdPO_4$ precipitation that is observed in, and may indirectly cause NSF. The new mechanism is also supported by no dissociation of dinuclear analog K_6[La_2(DTPA)$_2$(HPO_4)]·10H_2O (**6**) in solution, which shows no dissociation and only one set of ^{13}C NMR spectrum in Fig. 5.

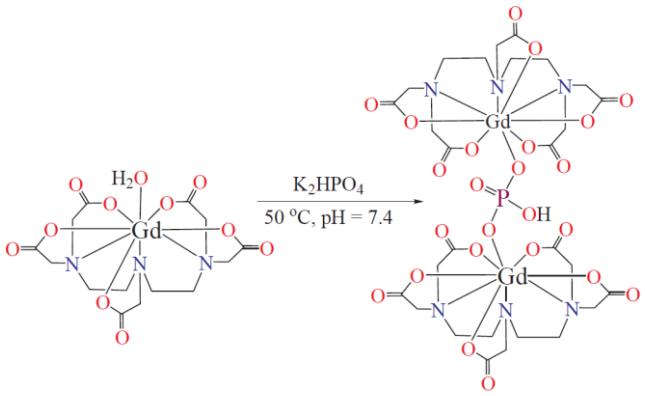

Sch. 1. Transformation of $[Gd(DTPA)(H_2O)]^{2-}$ to $[Gd_2(DTPA)_2(HPO_4)]^{6-}$ (**3**).

Finally, we note there is much recent interest in the literature in observations that gadolinium from GBCAs administered as part of MRI procedures can accumulate in tissues in individuals without renal deficiency and without obvious disease.[16] While the chemical form of this accumulated gadolinium is not yet known, if it turns out that the metal is no longer coordinated to its GBCA chelator, we point out that the mechanism proposed here may be more generally relevant to gadolinium accumulation in tissue, and not just the formation of the $GdPO_4$ deposits in NSF.

Conclusions

In conclusion, the substitutions of K_2HPO_4 and K_2HPO_3 with $K_2[Gd(DTPA)(H_2O)]\cdot 5H_2O$ (**1**) result in the formations of substituted phosphate and phosphite gadolinium products of $K_6[Gd(DTPA)(HPO_4)]\cdot 10H_2O$ (**2**) and $K_6[Gd_2(DTPA)_2(HPO_3)]\cdot 7H_2O$ (**3**). In the analogous reaction, the substituted lanthanum phosphite and phosphate were obtained for comparisons. Spectral and structural analyses indicate that the coordinated water molecule in $K_2[Gd(DTPA)(H_2O)]\cdot 5H_2O$ (**1**) was replaced by HPO_3^{2-} group to gives **2**, and by HPO_4^{2-} group to gives an undissociated mixed-ligand complex **3**. After the substitution, the complexation of DTPA with central Gd^{3+} cation becomes weaker. In GBCAs, the coordinated water molecules are able to be replaced by phosphate groups, leading to the weakening of the complexation of DTPA ligand with Gd^{3+}. This may well be the first step in the formation of gadolinium phosphate in NSF.

Acknowledgements

This work was supported by the Research Funds for the Central Universities (No. 20720150041), Natural Science Foundation of Fujian Province and the Program for Innovative Research Team in Chinese Universities (No. IRT_14R31).

Notes and references

1 (a) H. J. Weinmann, R. C. Brasch, W. R. Press, G. E. Wesbey, *Am. J. Roentgenol.*, 1984, **142**, 619−624; (b) D. H. Carr, J. Brown, G. M. Bydder, R. E. Steiner, H. J. Weinmann, U.Speck, A. S. Hall, I. R. Young, *Am. J. Roentgenol.*, 1984, **143**, 215−224.

2 (a) R. B. Lauffer, *Chem. Rev.*, 1987, **87**, 901−927;(b) P. Caravan, J. J. Ellison, T. J. McMurry, R. B. Lauffer, *Chem. Rev.*, 1999, **99**, 2293−2352; (c) J. C. Bousquet, S. Saini, D. D. Stark, P. F. Hahn, M. Nigam, J. Wittenberg, J. T. Ferrucci, *Radiology*, 1988, **166**, 693−698; (d) F. Cavagna, M. Dapra, F. Maggioni, C. Dehaen, E. Felder, *Magn. Reson. Med.*,1991, **22**, 329−333; (e) P. Wedeking, C. H. Sotak, J. Telser, K. Kumar, C. A. Chang, M. F. Tweedle, *Magn. Reson. Imaging*, 1992, **10**, 97−108; (f) C. A. Chang, *Invest. Radiol.*, 1993, **28**, S21−S27; (g) K. Adzamli, M. P. Periasamy, M. Spiller, S. H. Koenig, *Invest. Radiol.*, 1999, **34**, 410−414; (h) P. Caravan, *Accounts Chem. Res.* 2009, **42**, 851−862; (i) A. Datta, K. N. Raymond, *Accounts Chem. Res.*, 2009, **42**, 938−947.

3 P. Hermann, J. Kotek, V. Kubicek, I. Lukes, *Dalton trans.*,2008, **23**, 3027−3047.

4 (a) H. B. Na, I. C.Song, T. Hyeon, *Adv. Mater.*, 2009, **21**, 2133−2148;(b) A. K. Gupta, M. Gupta, *Biomaterials*, 2005, **26**, 3995−4021; (c) J. H. Lee, Y. M. Huh, Y. W. Jun, J. W. Seo, J. T. Jang, H. T. Song, S. Kim, E. J. Cho, H. G. Yoon, J. S. Suh, J. Cheon, *Nat. med.*, 2007, **13**, 95−99; (d) S. Laurent, D. Forge, M. Port, A. Roch, C. Robic, L. V. Elst, R. N. Muller, *Chem. Rev.*, 2008, **108**, 2064−2110; (e) B. Hamm, T. J. Vogl, G. Branding, B. Schnell, M. Taupitz, K. J. Wolf, J. Lissner, *Radiology*, 1992, **182**, 167−174; (f) B. Hamm, T. Staks, M. Tapuitz, R. Maibauer, A. Speidel, A. Huppertz, T. Frenzel, R. Lawaczeck, K. J. Wolf, L. J. Lange, *Magn. Reson. Imaging*, 1994, **4**, 659−668.

5 S. E. Cowper, H. S. Robin, S. M. Steinberg, L. D. Su, S. Gupta, P. E. LeBoit, *Lancet*, 2000, **356**, 1000−1001.

6 (a) T. Grobner, *Nephrol. Dial. Transplant.*, 2006, **21**, 1104−1108; (b) P.Marckmann, *J. Am. So. Nephrol.*, 2006, **17**, 2359−2362.

7 (a) A. S. Boyd, J. A. Zic, J. L. Abraham, *J. Am. Acad. Dermatol.*, 2007, **56**, 27−30; (b) W. A. High, R. A. Ayers, J. Chandler, G. Zito, S. E. Cowper, *J. Am. Acad. Dermatol.*, 2007, **56**, 21−26.

8 S. J. George, S. M. Webb, J. L. Abraham, S. P. Cramer, *Brit. J. Dermatol.*, 2010, **163**, 1077−1081.

9 (a) K. Kitajima, T. Maeda, S. Watanabe, Y. Ueno, K. Sugimura, *Int. J. Urol.*, 2012, **19**, 806−811; (b) J. M.Idee, N. Fretellier, C. Robic, C.Corot, *Crit. Rev. Toxicol.*, 2014, **44**, 895−913.

10 (a) T. Grobner, F. C. Prischl, *Kidney Int.*, 2007, **72**, 260−264; (b) A.Weller, J. L. Barber, Ø. E. Olsen, *Pediatr. Nephrol.*, 2014, **29**, 1927−1937; (c) V. C. Pierre, M. J. Allen, P. Caravan, *J. Biol. Inorg. Chem.*, 2014, **19**, 127−131; (d) J. X. Li, L. J. Fu, X. G. Yang, K. Wang, *J. Biol. Inorg. Chem.*, 2012, **17**, 375−385.

11 (a) L. Tei, Z. Baranyai, L. Gaino, A. Forgács, A. Vágner, M. Botta, *Dalton Trans.*, 2015, **44**, 5467−5478; (b) E. J. Bernstein, T. Isakova, M. E. Sullivan, L. B. Chibnik, M. Wolf, J. Kay, *Rheumatology*, 2014, **53**, 1613−1617; (c) S. Gao, M. L. Chen, Z. H. Zhou, *Dalton Trans.*, 2014, **42**, 639−645; (d) L. D. Besheli, S. Aran, K. Shaqdan, J. Kay, H. Abujudeh, *Clin. Radiology*, 2014, **69**, 661−668; (e) S. Faulkner, M. C. Carrie, Simon J. A. Pope, J. Squire, A. Beedy, P. G. Sammes, *Dalton Trans.*, 2004, **15**, 1405−1409.

12 (a) Y. X. Ni, J. M. Hughes, A. N. Mariano, *Am. Mineral.*,1995, **80**, 21−26;(b) H. Ettis, H. Naili, T. Mhiri, *Cryst. Growth Des.*, 2003, **3**, 599−602; (c) J. Zhu, D. W. Cheng, D. S. Wu, H. Zhang, Y. J. Gong, H. N. Tong, D. Zhao, *Cryst. Growth Des.*, 2006, **6**, 1649−1652.

13 G. K. Shimizu, R.Vaidhyanathan, J. M. Taylor, *Chem. Soc. Rev.*,2009, **38**, 1430−1449.

14 H. Gries, H. Miklautz, *Physiol. Chem. Phys. Med. NMR*, 1984, **16**, 105−112.

15 F. Poitrasson, E. Oelkers, J. Schott, J. M. Montel, *Geochim. Cosmochim. Acta*, 2004, **68**, 2207−2221.
16 R. J. McDonald, J. S. McDonald, D. F. Kallmes, M. E. Jentoft, D. L. Murrary, K. R. Thielen, E. E. Williamson, L. J. Eckel, *Radiology*, 2015, **273**, 772−782.

Graphic abstract

Commercial used gadolinium based contrast agents Gd-DTPA was substituted by phosphate and phosphite to form $K_6[Gd_2(DTPA)_2(HPO_4)]\cdot 10H_2O$ and $K_6[Gd_2(DTPA)_2(HPO_3)]\cdot 7H_2O$ respectively. Their analogous lanthanum complexes are compared that related to NSF formation.